Institutional Repository - Research Portal
Dépôt Institutionnel - Portail de la Recherche

researchportal.unamur.be

RESEARCH OUTPUTS / RÉSULTATS DE RECHERCHE

Simple approach to highly oriented ZnO nanowire arrays: large-scale growth, photoluminescence and photocatalytic properties

Xu, Fen Ma; Yuan, Zhong-Yong; Du, Gao-Hui; Ren, Tiezhen Yuan; Bouvy, Claire; Halasa, Matej; Su, Bao-Lian

Published in:
Nanotechnology

Publication date:
2006

Document Version
Early version, also known as pre-print

Link to publication

Citation for pulished version (HARVARD):
Xu, FM, Yuan, Z-Y, Du, G-H, Ren, TY, Bouvy, C, Halasa, M & Su, B-L 2006, 'Simple approach to highly oriented ZnO nanowire arrays: large-scale growth, photoluminescence and photocatalytic properties', *Nanotechnology*, vol. 17, no. 2, pp. 588-594.

Simple approach to highly oriented ZnO nanowire arrays: large-scale growth, photoluminescence and photocatalytic properties

Fen Xu[1], **Zhong-Yong Yuan**[1], **Gao-Hui Du**[2], **Tie-Zhen Ren**[1], **Claire Bouvy**[1], **Matej Halasa**[1] **and Bao-Lian Su**[1,3]

[1] Laboratory of Inorganic Materials Chemistry, The University of Namur (FUNDP), 61 rue de Bruxelles, B-5000 Namur, Belgium
[2] Electron Microscopy for Materials Research, University of Antwerp (RUCA), Groenenborgerlann 171, B-2020 Antwerp, Belgium

E-mail: bao-lian.su@fundp.ac.be

Abstract
A simple and low-cost soft route has been developed to the direct large-scale production of highly oriented ZnO nanowire arrays at 60 °C. It has been found that the growth of well-aligned ZnO nanowire arrays is dependent on several parameters, such as the reaction time and the concentration of ammonium ions. The environmentally benign ZnO nanowires obtained, with significant photoluminescence property and interesting photocatalytic activity, are single crystals and have a low defect concentration, which could be expected to find promising potential for optoelectronic and environmental application.

(Some figures in this article are in colour only in the electronic version)

1. Introduction

Since the first and very stimulating report of ultraviolet lasing from ZnO nanowires [1], the one-dimensional (1D) zinc oxide (ZnO) nanostructure [2] has been recognized as one of the most important multifunctional materials, because ZnO nanostructures can exhibit near-UV emission, optical transparency, electric conductivity, and piezoelectricity [3]. Owing to the fact that low-dimensional ZnO materials have great potential in sensors [4], optoelectronics [1], field emission [5], solar cells [6] and surface acoustic waveguides [7], substantial efforts have been devoted to the development of 1D ZnO nanostructures with novel methodologies and that of assemblies of 1D ZnO nanostructures.

Actually, 1D ZnO nanostructure assemblies can be fabricated by two principal methods: the evaporation and condensation processes (top-down strategy) [1, 3–11], and the solution-phase method (bottom-up strategy) [12–19]. Despite favouring high-quality 1D ZnO nanostructures and allowing their patterned growth, the commercial potential of gas-phase-grown ZnO nanowires remains constrained by the expensive equipment and the high energy-consumption of the process. Accordingly, liquid-phase approaches, also called 'chimie douce', to ZnO nanowire arrays are appealing due to their low growth temperature, versatile synthetic processes and great potential for scaling up. Notably, the various substrates used in the soft chemical route greatly facilitate the approach to 1D ZnO nanostructures with relatively low cost. For example, a thermal decomposition of a Zn(II) amino complex has been developed for fabricating ZnO micro/nanorod arrays on the various substrates and a seeded growth has been used to synthesize well-oriented ZnO nanorod arrays on a substrate coated with a layer of thin ZnO film or a metal layer [13–16]. The coating of the substrate with ZnO or metal thin film involves multistep procedures and seems to be a little complex.

---

[3] Author to whom any correspondence should be addressed.

Recently, Tang *et al* reported an interesting template-free aqueous route to grow ZnO nanorod arrays with the use of Zn foil as substrate by using a relatively high temperature (160–200 °C) and a concentrated oxidant (30% H_2O_2) [18]. Li *et al* used an attractive solution surface-erosion route at even room temperature to produce aligned ZnO nanorod arrays, using an organic oxidant (nitrobenzene) instead of H_2O_2 [19]. It remains a significant challenge to directly fabricate large-scale arrays of ZnO nanostructures with controlled orientation via a simple and low-temperature solution-based method.

Herein, we report a simple liquid-phase process to synthesize highly oriented arrays of single-crystalline ZnO nanowires on Zn foil under mild conditions, in which large-scale arrays of ZnO nanowires can be produced without any oxidant or organic agents at 60 °C. In contrast to many other techniques, strict substrate cleaning or preparation is not necessary, as long as there is no large debris such as dust or grease on the substrate surface. Besides the attractive low temperature, this simple growth of ZnO nanowire arrays may well avoid the use of exotic metals or metal oxides as catalyst or seed particles, because this process for the fabrication of ZnO nanoarrays would be through the self-seeding, continuous supply, and the subsequent anisotropic growth in the solution. The photoluminescence study reveals a strong UV emission, suggesting the potential light and field emission applications of these obtained ZnO nanowires. And the subsequent measurement of photocatalytic activity on organic compounds suggests that the obtained ZnO samples could have valuable activity in air and waste-water purification. This simple synthesis route not only would lead to the development of an effective and commercial growth process for well-oriented ZnO nanowires, but also be extendible to the production of highly oriented patterns of other oxide and sulfide nanomaterials.

2. Experiments

2.1. Synthesis of highly oriented ZnO nanowire arrays

The chemical reagents were purchased from Aldrich and used as received without further purification. Deionized water was used for all solutions in experiments. Typically, a 0.075 M $ZnSO_4$ aqueous solution (40 ml) containing NH_4Cl (molar ratio of $NH_4^+/Zn^{2+} = 20:1$) was first prepared, and its pH value was adjusted to ~11.7 with a NaOH solution (5 M). The resulting solution was transferred to a Teflon-lined autoclave. A $1 \times (1–1.5)$ cm^2 Zn foil (rinsed with deionized water several times before using) was suspended carefully in the solution followed by 12–15 h heating at a temperature of 60 °C. The foil was then removed from the solution, rinsed with deionized water and air-dried for further characterization.

2.2. Characterization

Scanning electron microscopy (SEM) images were carried out with a Philips XL-20 at 15–20 keV. Wide-angle x-ray powder diffraction (XRD) patterns were recorded on a Philips PW 1820 diffractometer using Cu Kα radiation. Transmission electron microscopy (TEM), high-resolution transmission electron microscopy (HRTEM) and selected area electron diffraction (SAED) were performed with a Philips CM30-FEG at 300 kV.

Electron energy-loss spectroscopy (EELS) was also recorded on a Philips CM30-FEG by using a Gatan image filtering (GIF) system. The photoluminescence (PL) was performed by a pulsed ArF laser ($\lambda = 193$ nm, pulse duration 8 ns, FWHM) at room temperature with a filter centred at 235 nm.

The photocatalytic activity experiments on the obtained ZnO nanowires for the decomposition of naphthalene in air were performed at ambient temperature. 11 mg of the obtained samples were removed from the Zn foil and then placed into 66 ml of saturated naphthalene aqueous solution (30 mg l^{-1}, water solubility [20]) in a tubular quartz reactor. The reactor was surrounded with six UV lamps (Osram Eversun, L40/79 K, 40 W). The reaction mixture was stirred under UV irradiation. The analysis of the residual naphthalene concentration in the reactor was performed with a PELS55-luminescence spectrophotometer ($\lambda_{ex} = 280$ nm, Xe lamp at room temperature). As a comparison, the photocatalytic activity of commercial ZnO powders (Aldrich, size <1 μm, 99.9%) was also tested at the same experimental conditions.

3. Results and discussion

3.1. Phase and morphology of the as-obtained ZnO nanowire arrays

Well-aligned ZnO nanowire arrays were fabricated via a simple liquid-phase approach. The general morphology of the products grown on the zinc foil was examined by SEM observation. The SEM image from the apical view (figure 1(a)) clearly shows that the surface of the Zn foil has been successfully coated with uniform-sized, densely packed and uni-oriented ZnO nanowires. The side-view SEM image with a higher magnification (figure 1(b)) reveals that every small quantity of nanowires seem to fuse and form bundle structures. The cross-section view of the arrays (figure 1(c)) indicates that the ZnO nanowires grow vertically at the surface of the Zn foil and penetrate into a thin layer (~180 nm) composed of nanocrystals. Usually, ZnO nanoparticle film is coated on the Si wafer or other substrates before the growth of ZnO nanoarrays. Thus, it would be desirable to make the nanoparticle layer as thin and continuous as possible, ideally a few particle diameters in extent ([14], Greene *et al*). A typical synthesis yields the ZnO nanowires with diameters of 150–200 nm and lengths of 5–6 μm.

The crystallinity of the nanowires and the orientation of growth were investigated by x-ray diffraction (XRD) and subsequent high-resolution transmission electron microscopy (HRTEM). The XRD pattern of the ZnO nanowire arrays on the zinc foil (figure 1(d)) exhibits a very sharp (002) diffraction line at 34.52° (FWHM: ~0.5°–0.6°) and a small (004) one at 72.62°, which illustrates the texture effect of the anisotropic morphology and the highly preferential orientation of the ZnO nanowires along the *c*-axis (perpendicular to the substrate surface). Other small diffraction lines, denoted by the stars (*), are assigned to the Zn foil (JCPDS card No. 04-0831, $P63/mmc$, $a = 2.665$ Å, $c = 4.947$ Å).

3.2. Structural characterization of the obtained products

TEM and HRTEM studies of ZnO nanowires removed carefully from the surface of Zn foil can provide further
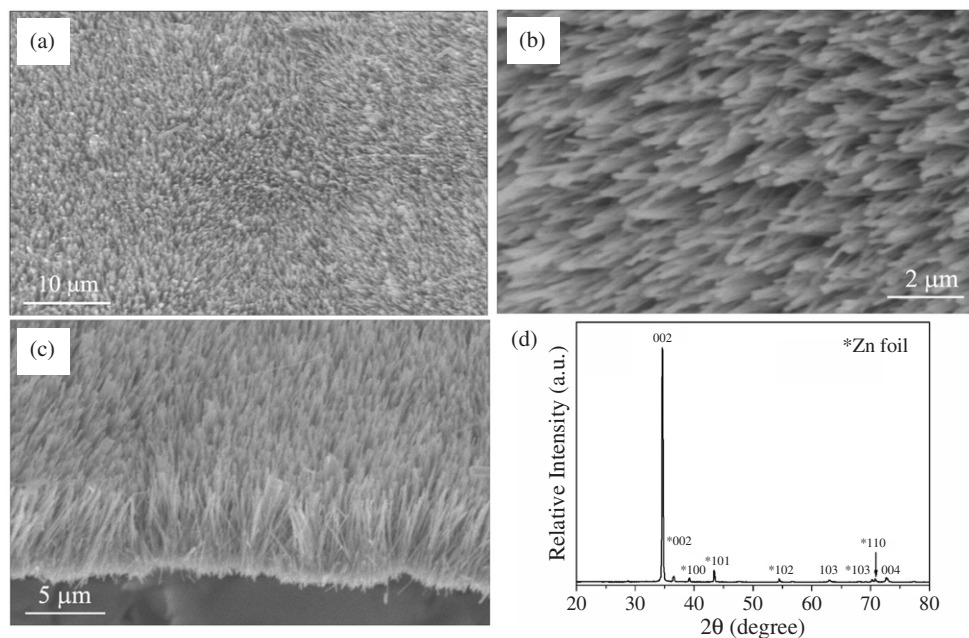
Figure 1. SEM images of aligned ZnO nanowires grown on a zinc foil: (a) apical view with low magnification; (b) side view with a higher magnification; (c) cross-section view; and (d) XRD pattern obtained from the arrays of ZnO nanowires on a zinc foil (the reflection lines indicated by * can be assigned to Zn foil).

insight into the morphology of these materials. Figure 2(a) is a TEM image, showing that the ZnO nanowires are very straight and have a uniform diameter along their axes. The HRTEM image presented in figure 2(b) indicates that the ZnO nanowire is single crystalline and its volume is free from dislocation. The lattice spacing of 0.52 nm corresponds to the *d*-spacing of the (0001) crystal planes, further confirming that ⟨0001⟩ is the preferential growth direction of these wurtzite-type ZnO nanowires. Additionally, the single-crystal nature of these nanowires and their ⟨0001⟩ growth direction have been demonstrated by the selected-area electron diffraction (SAED) pattern, which is recorded along the [1$\bar{1}$00] zone axis of the wurtzite-type ZnO crystals and shown in the inset of figure 2(a). The composition of the ZnO nanocone was analysed using electron energy loss spectroscopy (EELS), and figure 2(c) is a typical EELS spectrum recorded from a free-standing ZnO nanowire. The K edge of the oxygen is located at 534 eV, while the L_2 and L_3 edges of the Zn are located at 1043 and 1020 eV respectively. Only Zn and O elements are observed in the nanowire although the product is prepared in an ammonium salts solution, indicating the purity of the ZnO nanowires.

3.3. Influence factors: the growth time, Zn foil and NH_4^+ ions

The growth process of the oriented ZnO nanowire arrays was studied by SEM observation and the x-ray diffraction (XRD) technique. As shown in figure 3(a), the oriented nanostructures are not formed in the early stage of the crystal growth after 3 h hydrothermal treatment at 60 °C, in which ZnO nanoparticles with a diameter of 100–150 nm congregate to form a film with a thickness of around 180 nm. After 6 h growth at 60 °C (figure 3(b)), the initial characteristic of the desired nanostructures appears and many short rods are observed on

the surface of Zn foil, although most of these rods are not yet well aligned. Some ZnO nanorods, indicated by arrows, start to grow perpendicularly from the surface of the Zn foil. After 9 h treatment, a large number of nanowires, with diameters of 100–150 nm and lengths of 2–3 μm, grow in an oriented way and perpendicularly to the substrate (figure 3(c)). Upon increasing the growth time at 60 °C to 12 h, the average size of the nanowires increases up to 150–200 nm in width and 5–6 μm in length (figure 1(c)). Further increase of the reaction time has no obvious influence on the morphology and the size of the nanowires. A series of XRD patterns (figure 3(d)) confirmed that the initial ZnO nanocrystals are of hexagonal wurtzite phase (JCPDS card No. 36-1451, $P6_3mc$, $a = 3.249$ Å, $c = 5.206$ Å). Meanwhile, the XRD patterns of 3 and 6 h treatment samples are characteristic of randomly oriented ZnO nanostructures, in which the (101) reflection is the strongest line. With increasing growth time, the (002) reflection is significantly enhanced in the XRD pattern of 9 h material, confirming that the ZnO nanocrystals are mostly random at the initial stage but become well oriented along the ⟨0001⟩ direction after a long period of reaction.

Based on the SEM images and XRD patterns (figure 3), the growth of the aligned ZnO nanowire arrays appears to follow three formation steps; see Tian *et al* [14]. First, large quantities of ZnO nanoparticles form on the surface of zinc foil within 3 h, and the freshly formed nanoparticles can serve as the nuclei for the growth of ZnO nanocrystals. Second, many randomly oriented nanocrystals emerge gradually from these nanoparticles within 6 h. And finally, well-aligned nanowires form on prolonging the reaction time to 12 h. Additionally, the above-mentioned ZnO nanoparticle layer (shown in figure 1(c)) is possibly the remains of the early phase of the growth process.
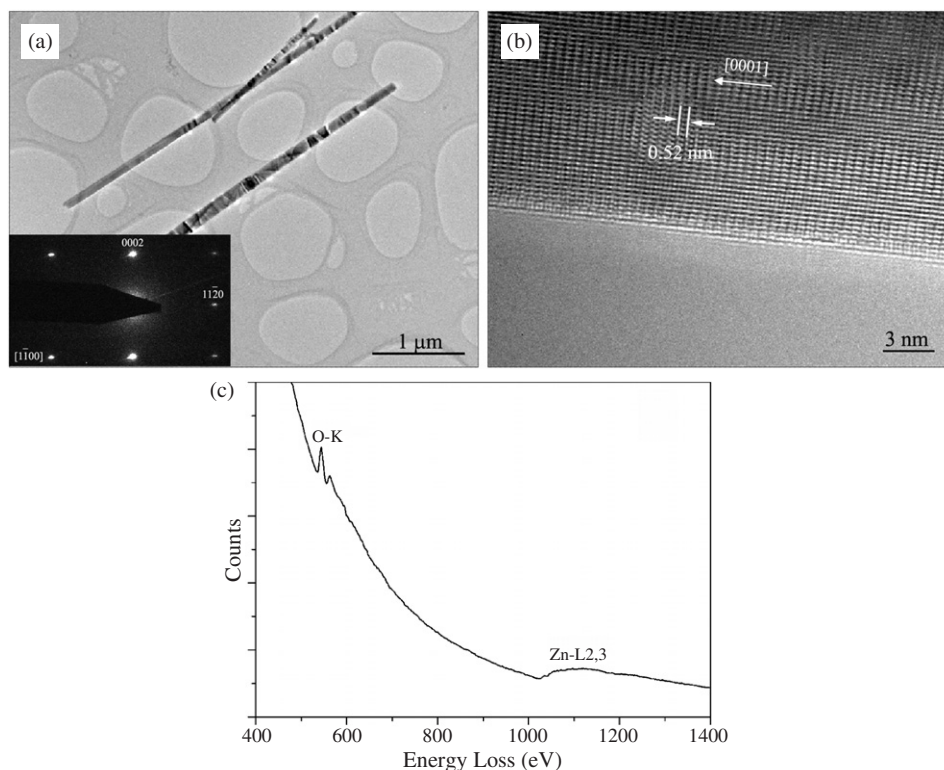
Figure 2. (a) TEM image of ZnO nanowires removed from the surface of zinc foil; the inset is the selected-area electron diffraction (SAED) pattern recorded along its [1$\bar{1}$00] zone axis; (b) HRTEM image; and (c) EELS spectrum of a ZnO nanowire.
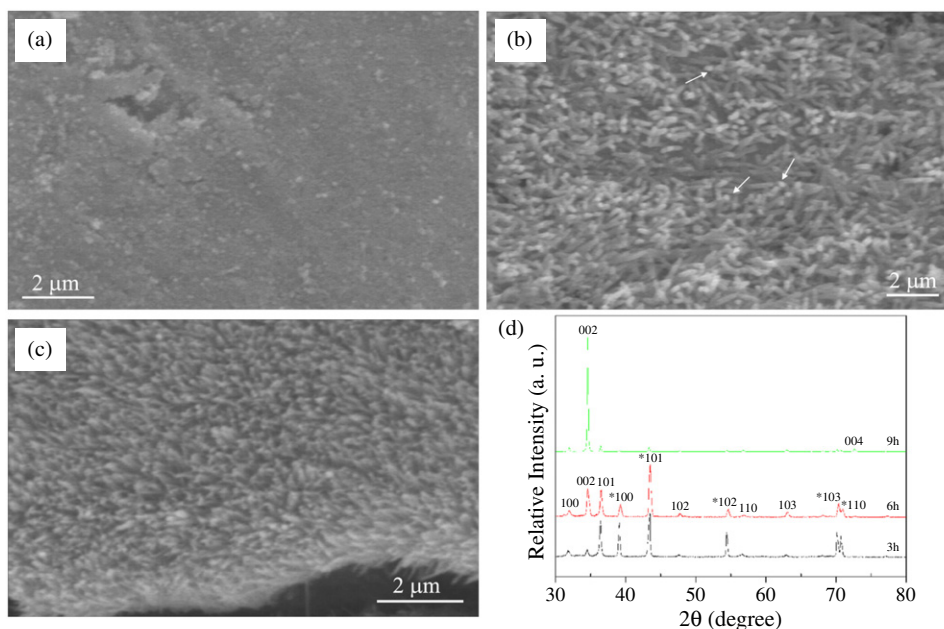

Figure 3. ZnO growth as a function of time. (a) ZnO seed-like particles on the zinc substrate after 3 h reaction. (b) Short ZnO rods appear after 6 h growth. Some ZnO nanorods, indicated by arrows, start to grow perpendicularly to the surface of the Zn foil. (c) Immature ZnO nanowire arrays form after 9 h growth. (d) XRD patterns of the ZnO nanostructure growth versus time.

Furthermore, when considering the formation of oriented ZnO nanowire arrays on a Zn foil, it should be mentioned that both Zn and ZnO have the same hexagonal structure with a relatively small lattice mismatch of 4.9 and 18.0% along the c and a axes, respectively, which might be sufficiently small for epitaxial growth [16, 17]. Default experiments in the absence of Zn foil show that ZnO nanowire arrays cannot be obtained under identical conditions. Therefore, it is thought

591

Table 1. The morphology of the obtained ZnO evolves with increasing NH_4^+/Zn^{2+} molar ratio, indicating the dependence of the nanowire growth on the NH_4^+/Zn^{2+} molar ratio.

NH^{4+}/Zn^{2+} (molar ratio)	0:1	10:1	20:1
The morphology of ZnO products	Dot-shaped nanocrystals	Nanorods with small aspect ratio	Nanowire arrays

that these ZnO nanocrystallites nucleate on the Zn foil and then preferentially develop along the [0001] direction to form 1D crystals under conditions in which the system constantly provides a ZnO source.

Moreover, the presence of NH_4^+ ions has a significant influence on the formation of the ZnO nanowire arrays. Here, the addition of NH_4^+ ions serves two proposes: advocating the formation of ZnO crystals and adsorbing on the polar surface of ZnO. It is well known that the generation of ZnO from Zn^{2+} ions usually needs organic agents, such as urea [21], formamide [21, 17], or hexamethylenetetramine [22, 13, 14] to complex with Zn^{2+} ions, and the subsequent aqueous thermal decomposition of Zn(II) organic complex supplies the necessary ZnO sources. In our case, Zn(II) is present in the form of $Zn(OH)_4^{2-}$ and/or $Zn(NH_3)_4^{2+}$ in the relatively strong basic solution and there are no organic complexing agents existent in the solution; thus NH_4^+ and/or $NH_3 \cdot H_2O$ species might be assumed to play a similar role in generation of ZnO from $Zn(OH)_4^{2-}$ and/or $Zn(NH_3)_4^{2+}$. Meanwhile, as regards wurtzite ZnO, an important characteristic of ZnO crystal is the polar surface, where the positive plane is rich in Zn atoms and the negative polar plane is rich in O atoms. The NH_4^+ ions would adsorb on the negative polar planes, i.e. $(10\bar{1}1)$, $(10\bar{1}0)$, and retard the growth rate of these planes, which has a significant effect on the morphology of the ZnO crystals. With the increasing concentration of NH_4^+ in the solution, NH_4^+ ions prefer to aggregate at more negative polar planes of ZnO crystals due to the electrostatic force, which would promote the growth along the [0001] direction greatly and result in the formation of nanowires with a higher aspect ratio. The effect of NH_4^+ ions as an orientation promoter can also be proved by a controlled experimental session, in which the molar ratio of NH_4^+/Zn^{2+} is adjusted from 0:1 to 10:1 while other parameters remain unchanged as presented above. Only dot-shape nanocrystals would be produced when just mixing Zn^{2+} with OH^- without NH_4^+ ions. And rod-shaped ZnO with small aspect ratio grow on the substrate when introducing a small quantity of NH_4^+ ions ($NH_4^+/Zn^{2+} = 10:1$), with some sign of the oriented growth. If the molar ratio NH_4^+/Zn^{2+} increases to 20:1, highly oriented arrays of ZnO nanowire will be formed (figure 1(c)). Table 1 summarizes the morphological transformation of the obtained ZnO products with the increase of the NH_4^+/Zn^{2+} molar ratio.

3.4. Optical and photocatalytic properties

Study of the photoluminescence (PL) spectrum is an effective technique to evaluate both ZnO defects and its optical property available as a photonic material. Figure 4 shows a typical room-temperature PL spectrum of high-quality ZnO nanowire arrays, where a strong UV emission at ∼384 nm dominates with a full width at half-maximum (FWHM) of about 30 nm. The strong emission at ∼384 nm (3.23 eV) originates from the annihilation of free excitons, whereas the well-known
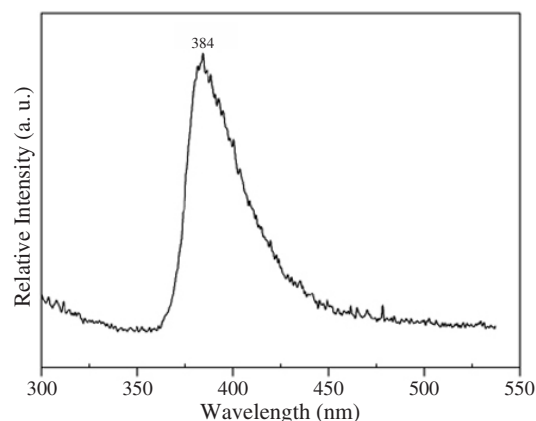
Figure 4. Room-temperature PL spectrum of the arrays of ZnO nanowires.

stronger and broader emission situated in the yellow–green part of the visible spectrum could not be registered. The bandgap of 3.23 eV estimated from the PL spectrum reduces noticeably when compared with the bulk ZnO (3.37 eV). According to our previous work on mesoporous TiO_2 [23], this may indicate that the obtained ZnO nanowires might be efficient in photocatalysis application, as shown in the following investigation. Furthermore, the sharp excitonic emission indicates that the ZnO nanowires have a low defect concentration and relevant optical properties [18].

Additionally, the preliminary photocatalytic testing revealed a much higher photocatalytic activity of naphthalene degradation over our as-prepared ZnO nanowires, in comparison with commercial ZnO powders (size <1 μm) measured under identical conditions. The photodecomposition of volatile organic compounds is an important application of environmentally friendly nanomaterials with controlled morphology for the 'green' treatment of waste water, because bioremediation through using living organisms is one of the most cost-effective technologies, but is also not as efficient as expected in the removal of polycyclic aromatic hydrocarbon (PAH) [24]. During the degradation of naphthalene over the as-obtained ZnO samples, the concentration of the naphthalene could significantly decrease to 1.93% after 30 min UV irradiation, then continue down to 0.37%–0.30% on prolonging the irradiation time to 45–60 min, respectively (figure 5(a)). However, as regards commercial ZnO powders, they need 105 min to decompose the naphthalene to 0.3% of the saturated concentration (figure 5(b)). For further comparison, figure 5(c) shows curves of the concentration of residual naphthalene with UV irradiation time over the as-prepared 1D ZnO nanowires and commercial ZnO powders. The enhanced photocatalytic property might be attributed to the high surface area and the nanofeatures [25], owing to the decreasing chance of recombination for photo-excited
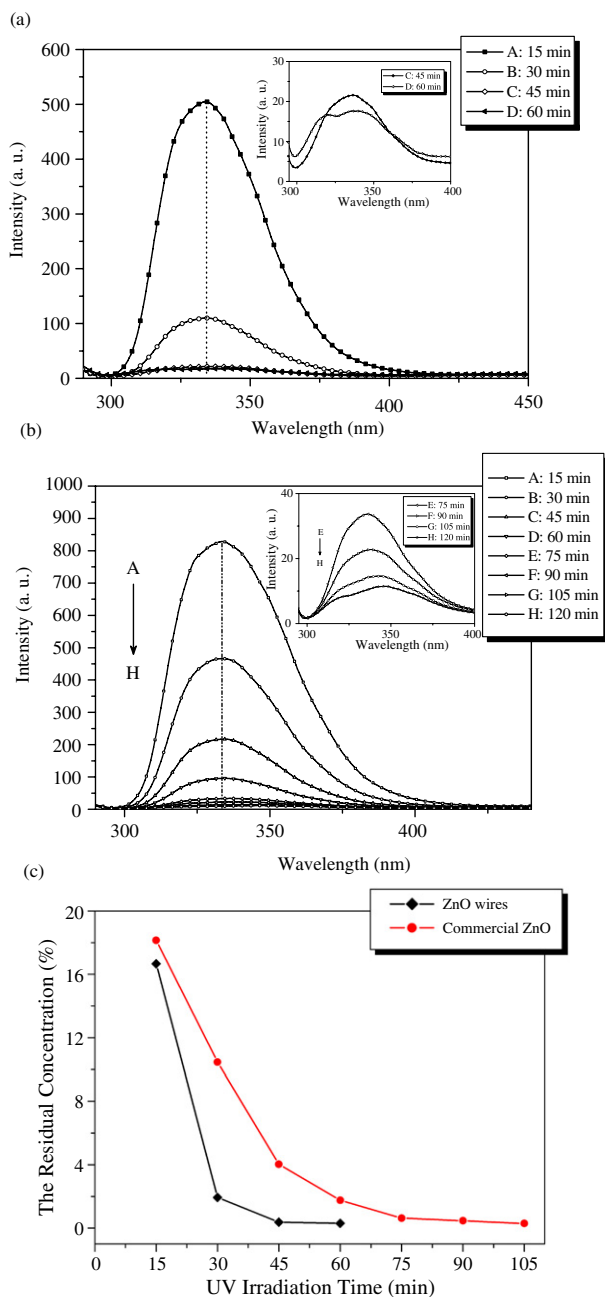
(a)

(b)

(c)

Figure 5. Room-temperature PL spectra ($\lambda_{ex} = 280$ nm) of naphthalene after UV irradiation over: (a) as-prepared ZnO nanowires; and (b) commercial ZnO powders, which indicates the naphthalene concentration decreases with the irradiation time. (c) Curves of the concentration of residual naphthalene with different UV irradiation time over the as-prepared ZnO nanowires and commercial ZnO powders.

electron–hole pairs [26]. The oxygen vacancies on the surface act as the capture centres for these electrons and thus restrain the recombination of electrons and holes. Moreover, because the holes attack the surface hydroxyls and yield surface-bound ·OH radicals [27], the surface hydroxyl groups can act as effective centres for photocatalytic reactions [28], Therefore, the photocatalytic activity of the ZnO nanowires is enhanced when compared to the ZnO powders. These preliminary results indicate that ZnO nanowire arrays could find promising

potential in environmental applications, such as air and waste-water purification.

4. Conclusions

In summary, highly dense arrays of ZnO nanowires can be fabricated on a large scale on a zinc foil by using a simple liquid-phase approach at 60 °C, without the assistance of oxidants and the use of exotic metals/metal oxides as catalyst or seed particles. The XRD patterns and SEM images illustrate the highly oriented arrays on the substrate. The interesting photoluminescence property of ZnO nanowires is recorded, revealing that our ZnO nanowires have a low defect concentration. Moreover, the preliminary measurement of the photocatalytic properties suggests that the obtained ZnO samples could have valuable potential in environmental and industrial applications. Such ZnO nanowire arrays could be expected to be a multifunctional component for solar cells, light emission, photonic, electronic and other devices.

Acknowledgments

References

[1] Huang M H, Mao S, Feick H, Yan H Q, Wu Y Y, Kind H, Weber E, Russo R and Yang P D 2001 *Science* **292** 1897
  Johnson J C, Yan H Q, Schaller R D, Haber L H, Saykally R J and Yang P D 2001 *J. Phys. Chem.* B **105** 11387
[2] Wang Z L 2003 *Nanowires and Nanobelts* vol I–II (Norwell, MA: Kluwer–Academic)
  Wang Z L, Kong X Y, Ding Y, Gao P X, Hughes W L, Yang R S and Zhang Y 2004 *Adv. Funct. Mater.* **14** 943
[3] Service R F 1997 *Science* **276** 895
  Kong X Y and Wang Z L 2003 *Nano Lett.* **3** 1625
  Wang X D, Summers C J and Wang Z L 2004 *Nano Lett.* **4** 423
[4] Minne S C, Manalis S R and Quate C F 1995 *Appl. Phys. Lett.* **67** 3918
  Shibata T, Unno K, Makino E, Ito Y and Shimada S 2002 *Sensors Actuators* A **102** 106
  Lin H M, Tzeng S J, Hsiau P J and Tsai W L 1998 *Nanostruct. Mater.* **10** 465
[5] Liu C H, Zapien J A, Yao Y, Meng X M, Lee C S, Fan S S, Lifshitz Y and Lee S T 2003 *Adv. Mater.* **15** 838
[6] Keis K, Vayssieres L, Lindquist S E and Hagfeldt A 1999 *Nanostruct. Mater.* **12** 487
[7] Gorla C R, Emanetoglu N W, Liang S, Mayo W E, Lu Y, Wraback M and Shen H 1999 *J. Appl. Phys.* **85** 2595
[8] Pan Z W, Dai S, Rouleau C M and Lowndes D H 2005 *Angew. Chem. Int. Edn* **44** 274
[9] Ng H T, Li J, Smith M K, Nguyen P, Cassell A, Han J and Meyyappan M 2003 *Science* **300** 1249
  Pan Z W, Dai Z R and Wang Z L 2001 *Science* **291** 1947
[10] Kong Y C, Yu D P, Zhang B, Fang W and Feng S Q 2001 *Appl. Phys. Lett.* **78** 407
  Lyu S C, Zhang Y, Ruh H, Lee H J, Shim H W, Suh E K and Lee C J 2002 *Chem. Phys. Lett.* **363** 134
  Wu J J and Liu S C 2002 *Adv. Mater.* **14** 215
  Park W I, Kim D H, Jung S W and Yi G C 2002 *Appl. Phys. Lett.* **80** 4232
[11] Zhang B P, Binh N T, Segawa Y, Wakatsuki K and Usami N 2003 *Appl. Phys. Lett.* **83** 1635

Li Y, Meng G W, Zhang L D and Phillipp F 2000 *Appl. Phys. Lett.* **76** 2011

Wu J J and Liu S C 2002 *J. Phys. Chem.* B **106** 9546

[12] Koh Y W, Lin M, Tan C K, Foo Y L and Loh K P 2004 *J. Phys. Chem.* B **108** 11419

Greene L E, Law M, Tan D H, Montano M, Goldberger J, Somorjai G and Yang P D 2005 *Nano Lett.* **5** 1231

[13] Feng X J, Feng L, Jin M H, Zhai J, Jiang L and Zhu D B 2004 *J. Am. Chem. Soc.* **126** 62

Vayssieres L 2003 *Adv. Mater.* **15** 464 and the reference therein

Choy J H, Jang E S, Won J H, Chung J H, Jang D J and Kim Y W 2003 *Adv. Mater.* **15** 1911

[14] Tian Z R R, Voigt J A, Liu J, Mckenzie B, Mcdermott M J, Rodriguez M A, Konishi H and Xu H F 2003 *Nat. Mater.* **2** 821

Greene L E, Law M, Goldberger J, Kim F, Johnson J C, Zhang Y F, Saykally R J and Yang P D 2003 *Angew. Chem. Int. Edn* **42** 3031

Peterson R B, Fields C L and Gregg B A 2004 *Langmuir* **20** 5114

[15] Yu H D, Zhang Z P, Han M Y, Hao X T and Zhu F R 2005 *J. Am. Chem. Soc.* **127** 2378

Hung C H and Whang W T 2004 *J. Cryst. Growth* **268** 242

Boyle D S, Govender K and O'Brien P 2002 *Chem. Commun.* 80

Li Q C, Kumar V, Li Y, Zhang H T, Marks T J and Chang R P H 2005 *Chem. Mater.* **17** 1001

Wang Z, Qian X F, Yin J and Zhu Z K 2004 *J. Solid State Chem.* **177** 2144

[16] Cui J B, Daghlian C P, Gibson U J, Rüsche R, Geithner P and Ley L 2005 *J. Appl. Phys.* **97** 044315

Hsu J W P, Tian Z R R, Simmons N C, Matzke C M, Voigt J A and Liu J 2005 *Nano Lett.* **5** 83

Tak Y and Yong K 2005 *J. Phys. Chem.* B **109** 19623

[17] Zhang Z P, Yu H D, Shao X Q and Han M Y 2005 *Chem. Eur. J.* **11** 3149

[18] Tang Q, Zhou W J, Shen J M, Zhang W, Kong L F and Qian Y T 2004 *Chem. Commun.* 712

[19] Li Z Q, Ding Y, Xiong Y J, Yang Q and Xie Y 2004 *Chem. Eur. J.* **10** 5823

[20] Gong Z Q, Alef K, Wilke B M and Li P J 2005 *Chemosphere* **58** 291

[21] Matijević E 1986 *Langmuir* **2** 12

[22] Vergies M A, Mifsud A and Serna C J 1990 *J. Chem. Soc. Faraday Trans.* **86** 959

[23] Ren T Z, Yuan Z Y and Su B L 2003 *Chem. Phys. Lett.* **374** 170

[24] May R, Schröder P and Sandermann H 1997 *Environ. Sci. Technol.* **31** 2626

Pagano J J, Scrudato R J, Roberts R N and Bemis J C 1995 *Environ. Sci. Technol.* **29** 2584

[25] Jiang L Q, Xu Z L, Sun X J, Shang J and Cai W M 2001 *Appl. Surf. Sci.* **180** 308

[26] Nosaka Y, Yamaguchi K, Miyama H and Hayashi H 1988 *Chem. Lett.* 605

[27] Richard C, Boule P and Aubry J M 1991 *J. Photochem. Photobiol.* **60** 235

[28] Bickley R I and Stone F S 1973 *J. Catal.* **31** 389